Available online at www.sciencedirect.com
SCIENCE DIRECT®
Journal of volcanology and geothermal research
ELSEVIER
Journal of Volcanology and Geothermal Research 129 (2004) 61–82
www.elsevier.com/locate/jvolgeores

Pressure changes associated with the ascent and bursting of gas slugs in liquid-filled vertical and inclined conduits

M.R. James [a,*], S.J. Lane [a], B. Chouet [b], J.S. Gilbert [a]

[a] *Department of Environmental Science, Institute of Environmental and Natural Sciences, Lancaster University, Lancaster LA1 4YQ, UK*
[b] *U.S.G.S., 345 Middlefield Road, MS 910, Menlo Park, CA 94025, USA*

Received 9 August 2002; received in revised form 3 October 2002; accepted 21 November 2002

Abstract

At basaltic volcanoes, the sources of long-period and very-long-period seismicity and acoustic signals are frequently described in terms of fluid dynamic processes, in particular the formation and ascent of gas slugs within the magma column and their bursting at the surface. To investigate pressure changes associated with these processes, two-phase flow experiments have been carried out in vertical and inclined pipes with both single gas slugs and a continuously supplied gas phase. The ascent of individual gas slugs is accompanied by strong dynamic pressure variations resulting from the flow of liquid around the slug. These dynamic transients generate sub-static pressures below the ascending slug in viscosity-controlled systems, and produce super-static pressures when the slug reaches the surface and motion ceases in inertia-dominated systems. Conduit inclination promotes a change of regime from bubbly to slug flow and favours an increase in size and velocity of the slugs at the expense of their frequency of occurrence during continuously supplied two-phase flow. The experimental pressure data support previous theoretical analyses of oscillatory sources in ascending slugs as the slugs approach the surface and burst. Pressure oscillations are also observed during the release of gas slugs and in their wake region.

Keywords: Strombolian-type eruptions; very-long-period seismicity; slug flow; pressure oscillations

1. Introduction

As commonly observed at Kilauea, Stromboli, and Etna volcanoes, the separation of exsolving gases from low-viscosity magmas can result in distinct styles of volcanic activity. These represent the surface expressions of different two-phase (magma and gas) flow regimes within the conduit, with Hawaiian eruptions being the result of annular flow and Strombolian eruptions representing the bursting of large individual gas bubbles. As the repeatability of many long-period (LP, 0.2–2 s) and very-long-period (VLP, 2–100 s) seismic events recorded at basaltic volcanoes suggest, they have non-destructive, fluid dynamic sources (Chouet, 1988; Chouet et al., 1994; Neuberg et al., 1994; Chouet, 1996; Chouet et al., 1997, 1999; Ripepe and Gordeev, 1999; Ripepe et al.,

* Corresponding author. Tel.: +44-(0)1524-65201; Fax: +44-(0)1524-593985.
E-mail addresses: m.james@lancaster.ac.uk (M.R. James), s.lane@lancaster.ac.uk (S.J. Lane), chouet@usgs.gov (B. Chouet), j.s.gilbert@lancaster.ac.uk (J.S. Gilbert).

0377-0273/03/$ – see front matter © 2003 Elsevier B.V. All rights reserved.
doi:10.1016/S0377-0273(03)00232-4

2001; Chouet et al., 2002; Konstantinou, 2002). An understanding of these processes is becoming increasingly important. LP events are commonly believed to represent the result of resonating source regions (Chouet, 1988, 1992, 1996; Kumagai and Chouet, 1999) whereas VLP events are attributed to the wholesale movement of liquid (Arciniega-Ceballos et al., 1999; Nishimura et al., 2000; Kumagai et al., 2001; Chouet et al., 2002). In this study, we carry out pressure measurements on two-phase laboratory flows in pipes to gain further insights into how large ascending bubbles can act as sources of seismic and acoustic energy.

At Stromboli, both tremor and eruption seismic signals have been associated with bubble coalescence and rise (Chouet et al., 1997, 1999; Ripepe and Gordeev, 1999; Ripepe et al., 2001; Chouet et al., 2002), and infrasonic acoustic measurements have been modelled with processes associated with bubbles bursting at the surface of the lava column (Vergniolle and Brandeis, 1996; Ripepe and Gordeev, 1999). Recent work on VLP seismic data from Stromboli points to highly repeatable source mechanisms associated with explosions (Chouet et al., 1999, 2002). The locations of these sources, offset from directly under the vent region, suggest a conduit inclined roughly 30° from the vertical, rising from a depth of about 200 m below the surface (Chouet et al., 2002). The inclination of the conduit has implications not only for the stability of the flow regimes likely to occur within it, but also for the details of how these flow regimes are expressed. Accordingly, the experiments described here were carried out in both vertical and inclined tubes in order to investigate the dependence of flow patterns on tube inclination and quantify the resulting pressure fluctuations within the flow.

Engineering applications such as transport pipelines and bubble column reactors have driven a comprehensive literature on two-phase (gas–liquid) flows in pipes, although much work remains to be done to achieve full understanding of the complexities of the fluid dynamics involved (Joshi, 2001). A considerable amount of this literature describes details of the slug flow regime (believed to be responsible for Strombolian eruptions (Blackburn et al., 1976; Seyfried and Freundt, 2000) at basaltic volcanoes) in which large bubbles with diameters approaching that of the pipe, rise within a continuous liquid phase. In engineering, this regime is usually described by using the terms 'Taylor bubble' for the gas phase and 'liquid slug' for the connected, liquid phase. However, we retain here the terminology commonly used in the volcanology literature (Jaupart and Vergniolle, 1989; Seyfried and Freundt, 2000; Ripepe et al., 2001) and by Clift et al. (1978), in which the gas phase is referred to as the slug. Detailed two-phase flow studies have focused on the bubbly to slug flow regime transition (Legius et al., 1997; Cheng et al., 1998; Krussenberg et al., 2000), slug ascent velocity (Nicklin et al., 1962; White and Beardmore, 1962; Zukoski, 1966; Wallis, 1969; Seyfried and Freundt, 2000; Shosho and Ryan, 2001), coalescence of slugs (Shemer and Barnea, 1987; Pinto and Campos, 1996), and the documentation of slug shapes (Gopal and Jepson, 1998; Polonsky et al., 1999a; Seyfried and Freundt, 2000) and liquid flow patterns around slugs (Kawaji et al., 1997; Polonsky et al., 1999b; Bugg and Saad, 2002).

Three dimensionless parameters are required to compare gas slugs rising buoyantly in liquid-filled tubes in different systems (White and Beardmore, 1962). These are the Froude number:

$$Fr = \frac{U_o}{\sqrt{gD}} \tag{1}$$

Morton number:

$$Mo = \frac{g\mu^4}{\rho\sigma^3} \tag{2}$$

and Eötvös number:

$$Eo = \frac{\rho g D^2}{\sigma} \tag{3}$$

where U_o represents the terminal ascent velocity of the slug, g is the gravitational acceleration constant, D is the internal diameter of the tube, and μ, ρ, and σ are the viscosity, density, and surface tension of the liquid, respectively. Within the space defined by these parameters there exists a region within which viscous and surface tension forces are trivial (White and Beardmore, 1962). In

this region, bounded by $Mo < 10^{-6}$ and $Eo > 100$ (White and Beardmore, 1962), slugs are inertially controlled and rise at their maximum velocity in vertical tubes, given by $Fr = 0.35$. Zukoski (1966) demonstrated that slugs rising in inclined tubes can exceed this velocity by up to $\sim 80\%$.

In basaltic systems with vertical conduits, typical ranges of these parameters are $0.1 < Fr < 0.35$, $10^5 < Eo < 10^7$, and $10^5 < Mo < 10^{10}$, assuming $50 < \mu < 500$ Pa s, $\rho = 2600$ kg m^{-3} and $\sigma = 0.4$ N m^{-1} for basalt, and $1 < D < 10$ m for the conduit (Seyfried and Freundt, 2000). These ranges indicate that gas slugs ascend within a transitional regime with a velocity dependent on slug volume and liquid viscosity. When $Eo > 100$, the surface tension plays little role in determining the slug ascent velocity (Wallis, 1969). In the experiments described here, $D = 0.038$ m, $0.16 < U_o < 0.33$ m s^{-1}, $0.001 < \mu < 0.9$ Pa s, and $\sigma \approx 0.07$ N m^{-1}, which place the flows within the inertial and transitional regimes with $0.26 < Fr < 0.54$, $200 < Eo < 270$, and $10^{-11} < Mo < 14$ (Table 1). As the diameter of our laboratory-scale pipe dictates a much smaller Eötvös number than in basaltic systems, surface effects will be enhanced in our experiments, but should not represent a controlling factor.

To assess the importance of viscous effects, a dimensionless inverse viscosity:

$$N_f = \left(\frac{Eo^3}{Mo}\right)^{\frac{1}{4}} = \frac{\rho D^{\frac{3}{2}} g^{\frac{1}{2}}}{\mu} \quad (4)$$

may also be considered (Fabre and Liné, 1992), in which the viscous regime is given by $N_f < 2$, and inviscid approximations are appropriate for $N_f > 300$. For the parameters given above for a basaltic system, $16 < N_f < 5000$ while, in our laboratory flows, $34 < N_f < 30\,000$. It is worth noting that in the inviscid case, where slugs are inertially controlled, the condition $Fr = 0.35$ implies that N_f becomes proportional to the Reynolds number, Re, defined as $Re = \rho UD/\mu$. Reynolds numbers for slugs in our experiments vary between ~ 10 and 10^4. For a basaltic system and assuming slug rise velocities of order 1 m s^{-1}, $5 < \mathrm{Re} < 10^3$. Therefore, our experiments cover relevant regimes, with end members under inertial control and approaching viscous control. Processes suggested by our pressure measurements should therefore be scalable to basaltic systems.

2. Apparatus

Our experiments were carried out using a tube of borosilicate glass with internal diameter of 38 mm (Fig. 1). In experiments with vertical tubes, the apparatus was suspended from its top end using a rubber bicycle inner tube to isolate the tube from external vibrations. In experiments with inclined tubes, the bicycle inner tube was disconnected from the top of the tube and looped through a chain attached at two different points along the tube. Pressure sensors were mounted in the base of and at various intervals along the experimental tube with the sensor inlets set flush with the inside surface of the tube. Two different types of pressure sensor were used, namely BOC Edwards Active Strain Gauges (ASGs) and Honeywell differential pressure sensors 163PC01D75 (163PCs). The ASG pressure sensor has a frequency range of d.c. to ~ 1 kHz and an absolute accuracy of ± 400 Pa. The 163PC sensor measures the difference of pressure between the 'wet' sensing inlet and pressure outside the tube (i.e. atmospheric pressure), and has a dynamic range of ± 800 Pa and quoted response time of 1 ms. How-

Table 1
Typical values of dimensionless constants for slug ascent in vertical tubes during the experiments

Experimental liquid	Viscosity	Dimensionless number					Observed control
	(Pa s)	*Fr*	*Mo*	*Eo*	N_f	*Re*	
Water	0.001	0.35 (0.54)	10^{-11}	200	10^4	$\sim 10^4$	inertial
Sugar 1	0.09	0.29 (0.47)	10^{-3}	250	320	95 (145)	transitional
Sugar 2	0.9	0.26 (0.33)	14	270	34	9 (11)	viscous

Where they differ significantly, typical values for tubes inclined at 40° are given between parentheses.

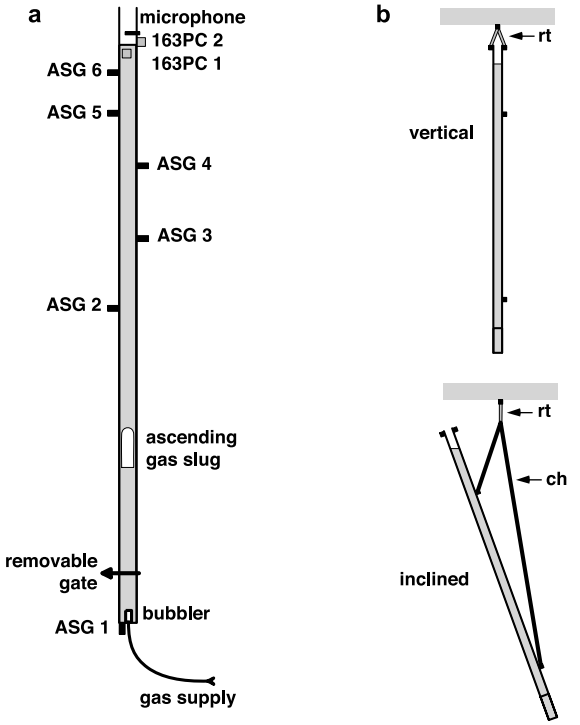

Fig. 1. Experimental apparatus consisting of a 2.5-m-long liquid-filled glass tube. (a) Apparatus setup. Pressure sensors (ASG transducers) are located along the tube, and smaller-range 163PC differential pressure transducers are set up close to or just above the liquid surface. A removable gate is used for slug generation during single slug experiments. This gate is omitted during continuous gas-supply experiments, during which gas enters the liquid column from a bubbler set in the base of the tube. (b) Tube mounting configurations. In experiments carried out with a vertical tube, the tube is suspended from a concrete ceiling using rubber tubing (rt). In experiments with inclined tubes, the tubing is connected to a chain (ch), which is attached at two different points to the experimental tube. The angle of the tube is varied by altering the length of chain on either side of the suspension point and the tube is tilted counterclockwise within the plane of the sketch shown in (a), so that transducers ASG 3, ASG 4, and 163PC2 are located on the upper wall of the tube.

ever, unexplained phase differences observed in some of the data recovered from these sensors at frequencies higher than 100 Hz (possibly resulting from slight contamination of the semi-conducting sensing wafer) suggest that a slower response time of 0.01 s may better characterise such transducers. A microphone AKG CK 77 WR, with flat response between 200 and 10 kHz (−1 db at 100 Hz, −8 db at 30 Hz), was also used to record acoustic signals above the liquid column.

Output voltages from the sensors were logged at a sampling rate of 5 kHz with 16-bit resolution using a National Instruments DAQ board in a PC. Experiments were also recorded with a digital video camera (Canon DM-XL1 in FRAME mode) synchronised to the pressure data by including an LED binary counter (incremented by the scan clock of the logging board) within the field of view. Using a shutter speed of 1/1000 s, the digital images could be correlated to the sensor data with an accuracy of ±5 data points (1 ms).

Two different kinds of experiments were carried out, in which air was the gas phase and sugar–water solutions were used for the liquid phase. Tap water was used as the lowest-viscosity liquid (0.001 Pa s). To obtain more viscous liquids, white cane sugar was dissolved in tap water to produce solutions with viscosities of 0.09 and 0.9 Pa s, and densities of 1250 and 1320 kg m^{-3}, respectively (Table 1). The rise of single gas slugs was investigated in the three liquids over a range of tube inclinations. Gas slugs were produced by using a gate made of either a Teflon or copper sheet set in a joint located 20 cm above the base of the tube (Fig. 1). The upper portion of the tube was then filled with liquid up to a height of about 2 m, leaving the lower section dry. Rapid removal of the gate released the gas slug. To minimise oscillations of the liquid column induced during release of the slug, the gas section was pressurised to hydrostatic pressure prior to slug release. Unfortunately, difficulties in producing a perfectly gas-tight seal at the gate (particularly when the tube was inclined) made it difficult to completely eliminate such transient oscillations. The nominal mass of gas in a slug was 0.3 g.

Further experiments were carried out in which a constant supply of gas was injected via either a wooden or ceramic bubbler (fish tank aerators) at the base of the tube, and pressure changes were measured during the continuous rise of the bubbles and developing gas slugs produced in that manner. These experiments were conducted over a range of tube inclinations and two liquid viscos-

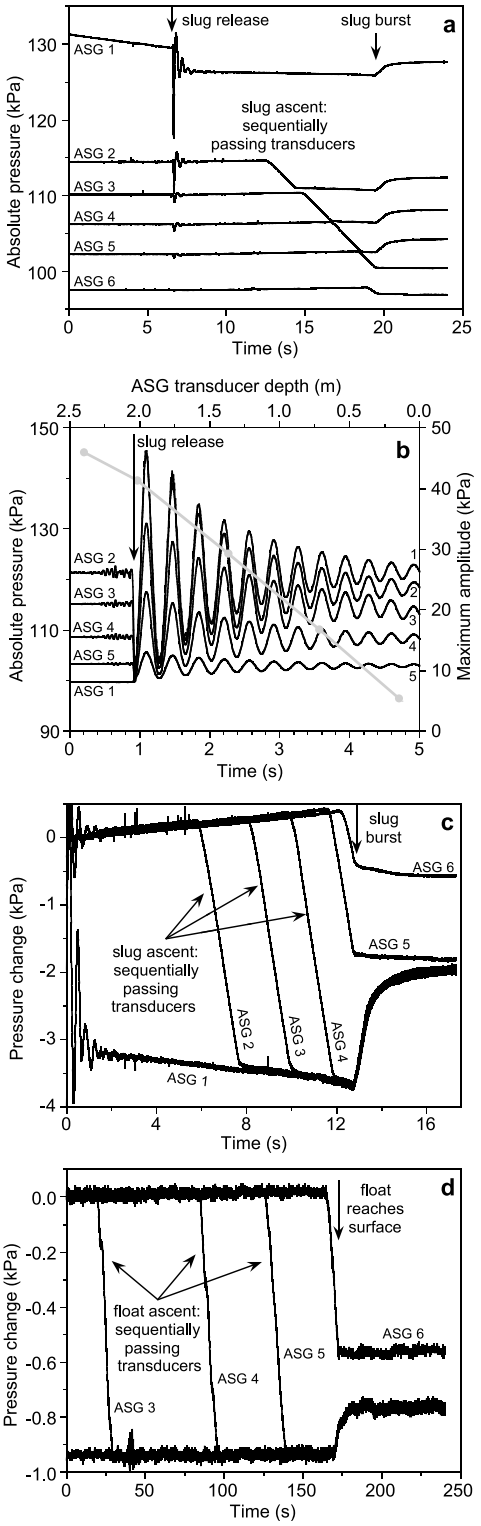

ities (0.001 and 0.09 Pa s). The pressurised gas was provided by a regulated air cylinder to minimise oscillations generated by the source.

3. Experiments with single gas slugs

Characteristic pressure changes induced during the ascent of individual gas slugs were observed in all our experiments. The behaviour of the pressure fluctuations was found to depend on both the liq-

Fig. 2. Pressure changes recorded by the ASG sensors during the ascent of a gas slug or rise of a buoyant float. (a) Absolute pressures recorded during the ascent of a slug in liquid with a viscosity of 0.9 Pa s. Pressure equalisation of the slug was carried out before slug release. The slope of the ASG 1 data before slug release is the result of gas loss from the slug source caused by a slightly leaky gate, however, the slug was still slightly above static pressure when it was released as shown by the relatively large pressure drop. The oscillations near 7 s are caused by vibrations of the apparatus and liquid column triggered at the withdrawal of the gate retaining the slug. Upon reaching the surface of the liquid near 19 s, the slug bursts, leaving the upper sensors (ASG 5 and 6) no longer immersed in liquid. (b) Results obtained for a slug under atmospheric pressure released in a liquid with viscosity of 0.001 Pa s. Note that the individual pressure traces are labelled on both the left- and right-hand side of the plot. Without pressure equalisation, the vertical oscillations of the liquid column induced by the release of the slug are responsible for the large dynamic pressures recorded. With the exception of ASG 1 located at the base of the tube beneath the slug, the maximum amplitude of pressure oscillations, indicated by the grey line with symbols and measured by the right-hand scale, is directly proportional to the pressure transducer depth. The pressure changes recorded during the slug ascent and bursting in (a) are clarified in (c), where the static pressure immediately after slug release has been subtracted from the data of each sensor. As the slug ascends and expands, sensors above it detect an increased pressure due to the increasing head of water. Sensors below the slug detect a gradually decreasing pressure due to the increasing magnitude of dynamic losses in the flowing liquid around the expanding slug. After the slug bursts, a gradual flow of liquid returns the pressure values to their new static pressures (which are lower than the initial static pressures due to the volume below the gate now being occupied by liquid). For comparison with (c), the data shown in (d) represent the ascent of an incompressible float in the same liquid (0.9 Pa s). These data demonstrate the absence of the pressure changes associated with the expansion of the slug as it ascends the tube.

uid viscosity and tube inclination. In order to demonstrate the main features of the pressure changes recorded, Fig. 2a shows the ASG data from an experiment carried out with a vertical tube and a liquid viscosity of 0.9 Pa s. These data represent absolute pressures, therefore their offsets are representative of the different heads of liquid above individual sensors. At 0 s the data represent the hydrostatic pressure at each sensor before the slug is released, and at 25 s the data reflect the decreased hydrostatic pressures after the slug has burst. During intermediate times, the pressure data represent the contributions from both hydrostatic pressure and dynamic pressure variations associated with liquid movements. These pressure changes, and variations in them due to liquid viscosity and tube inclination, are discussed below for the time intervals including the slug release, slug rise, slug approaching the surface, and slug bursting.

3.1. Slug release

The transient oscillations detected near 7 s (Fig. 2a) are due to vibrations of the apparatus and water column induced during slug release. Pressure equalisation of the gas slug was carried out before its release, therefore static pressures measured above the slug do not change rapidly and these transients mainly reflect the accelerations of the apparatus and liquid column induced by the physical removal of the gate. Several experiments were also carried out during which the gas was left at atmospheric pressure before release. Data collected during these experiments displayed much larger pressure oscillations (Fig. 2b) induced by the water column bouncing on the gas slug after its release. These dynamic pressure oscillations reflect the acceleration of the liquid column, as demonstrated by the increasing magnitude of pressure oscillation with increasing sensor depth (shown by the grey line and symbols in Fig. 2b). At the base of the column, the pressure increase required to accelerate all the liquid above it must be significantly larger than the pressure increase measured near the surface of the liquid, where only a small amount of pressure is required to accelerate a comparatively smaller mass of liquid. Above the slug and in a liquid of constant density, just as the hydrostatic pressure is proportional to depth, the amplitudes of dynamic pressure oscillations are also proportional to depth. Below the slug, in contrast with hydrostatic pressure, amplitudes are constant with depth. With a greater liquid viscosity, the oscillation amplitude would be reduced from those shown in Fig. 2b due to the smaller accelerations of the liquid.

3.2. Slug ascent

After the removal of the gate, the slug rises past the pressure sensors, which sequentially detect a pressure drop as a result of the decreased mass above them (Fig. 2a). The roughly linear pressure drop recorded during the interval 12–19 s by sensors ASG 2–5 marks the passage of the body of the slug past each transducer. However, as indicated by the subsequent pressure increase back to hydrostatic when the slug bursts near 19 s, some of the pressure drop must also reflect a dynamic effect associated with the liquid flowing around the gas slug. The pressure increase near 19 s reflects the termination of this dynamic effect and gradual slumping of the liquid film from around the sides of the burst bubble, back to the top of the liquid column.

Dynamic effects are more obvious in Fig. 2c, where the initial hydrostatic pressure immediately following slug release has been subtracted from the data. These results show the pressure changes detected by each sensor during slug ascent and slug burst. A steady pressure increase is detected before the slug reaches a transducer, and a gentle pressure decrease is observed after the slug has completely passed by the transducer. Finally, the pressure increases again after the slug has burst at the surface of the liquid. Final static pressures are lower than those recorded at the beginning of the experiment, reflecting the lower level of liquid in the tube as the liquid now fills the volume originally occupied by gas below the gate.

As the gas slug rises in the tube, it expands in response to the decreasing static pressure it experiences (Polonsky et al., 1999a; Seyfried and Freundt, 2000). Consequently, the surface of the

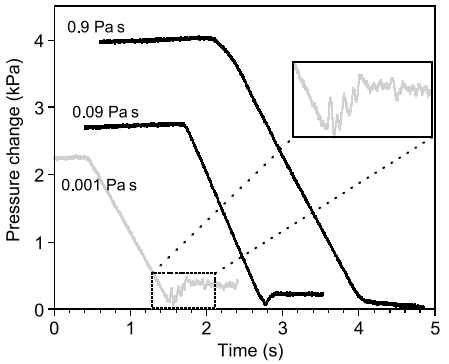

Fig. 3. Pressure changes observed in the wakes of slugs ascending in liquids of different viscosities. In tap water (0.001 Pa s), the wake immediately behind the slug (expanded in the inset box) shows a low-pressure signal lasting ~400 ms and representing a length scale of ~2.3*D*. During this interval, pressure oscillations are measured in coincidence with the visually observed turbulent nature of the slug wake. In a sugar solution with viscosity of 0.09 Pa s, the reduced pressure region is still present, however, no oscillations are detected. In a sugar solution with viscosity of 0.9 Pa s, the reduced pressure region and oscillations are both absent. For a liquid at this viscosity, the wake region is not observed to be turbulent.

water column must rise and the pressure sensors above the slug detect the increased water head above them. This results in a steady increase of pressure before the slug reaches a transducer (Fig. 2c). Following the passage of the slug past the transducer (indicated by the sharp pressure decrease), the pressure measured by this sensor continues to gradually decrease until the slug bursts at the surface. This non-intuitive behaviour is the result of dynamic losses within the fluid film flowing past the sides of the rising slug due to the liquid viscosity. As the slug ascends and expands, the increasing slug length increases the magnitude of this effect, which manifests itself in the gradual pressure decreases measured below the slug (Fig. 2c).

These interpretations are supported by the data in Fig. 2d, which show results obtained in an experiment in which the gas slug was replaced by an incompressible float (a 101-mm-long cylinder with a diameter of 31 mm and mass of 10.5 g). The results in Fig. 2d are qualitatively similar to those in Fig. 2c, but lack the subtle pressure changes associated with the expansion of a rising gas slug. For example, sharp pressure decreases are observed as the float passes each sensor, and pressure increases are seen in association with the cessation of liquid flow after the float has reached the surface. However, the gradual pressure changes due to increasing liquid head and increasing slug length are not present.

Detailed observations of the pressure changes immediately behind ascending slugs show that the wake region varies with liquid viscosity. Visual observations indicate that slugs rising in water are trailed by a turbulent wake containing many entrained small bubbles. In this case, the shape of the slug base is constantly changing. This wake effect is demonstrated in the pressure data illustrated in Fig. 3. In a liquid with viscosity of 0.001 Pa s, the passage of the slug is followed by a short interval of low pressure. Pressure oscillations observed within this low-pressure interval reflect the turbulent nature of the bubble wake. In contrast, no low-pressure interval is detected behind slugs rising in a 0.9-Pa-s liquid. In a liquid of intermediate viscosity (0.09 Pa s), the transient pressure decrease is still observed but the pressure oscillations are absent.

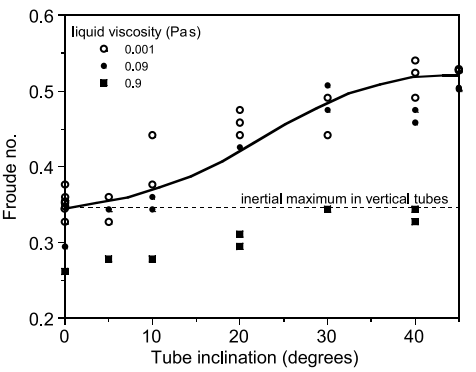

Fig. 4. Dependence of the slug ascent velocity on tube inclination and liquid viscosity. The velocity is given in dimensionless form by the Froude number. The solid curve shows the empirical fit obtained by Zukoski (1966) for slugs ascending in vertical and inclined tubes filled with an inviscid liquid. The results from our 0.001 and 0.09 Pa s solutions are similar, indicating that slugs in our experiments were rising close to this inertial regime. Velocities are considerably reduced in a 0.9-Pa-s solution, suggesting that viscosity is increasingly controlling slug ascent in higher-viscosity liquids. The inertial maximum of $Fr = 0.35$ for vertical tubes (White and Beardmore, 1962) is indicated by the dashed line.

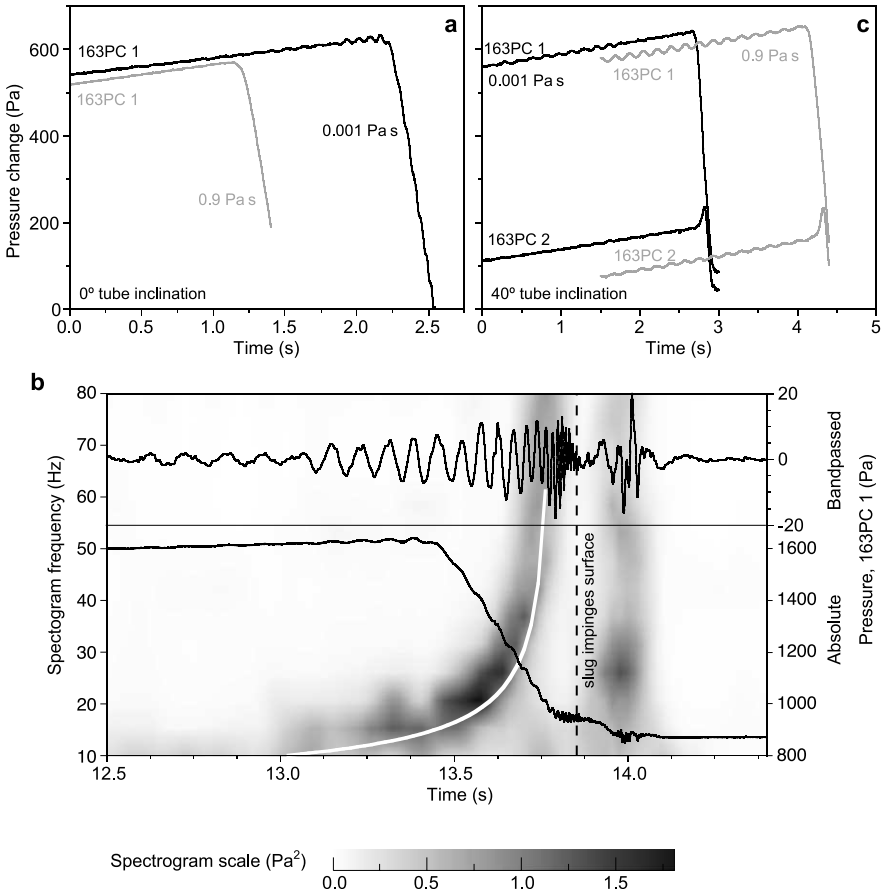

Fig. 5. Pressure oscillations detected as a slug approaches the liquid surface. (a) Data for vertical tubes. Increasing oscillation amplitudes are observed in the 163PC data above the slug only in a low-viscosity (0.001 Pa s) liquid (only 163PC 1 data shown). (b) Raw pressure data (lower trace), and band-pass filtered (7–100 Hz band) pressure (upper trace). The spectrogram (0.2-s window sliding in increments of 0.02 s across the record) shows the frequency increase detected as the slug approaches the surface. The white line superimposed on the spectrogram represents the frequency of longitudinal oscillations of the gas slug estimated from Eq. 7, see text). (c) Data for tubes inclined at 40°. The more pronounced oscillations are believed to be an experimental artefact. The increasing oscillation amplitudes seen in (a) as the slug approaches the surface are not observed in this case. Note the small pressure spike in front of the slug on the upper wall of the tube (163PC 2 data).

Slug ascent velocities were determined from video records. Measurements were made in the top 30 cm of the tube, and the results are represented by Froude numbers for different tube inclinations and liquid viscosities (Fig. 4). The scatter in the data displayed in Fig. 4 primarily reflects the fact that the apparatus was not optimised for velocity measurements. In particular, the pressure sensor mounting brackets obscured sections of the tube, thus reducing the area of the video frames available for analysis. Despite such limitations, our data are found to be comparable with previously published results (Zukoski, 1966) and are presented here to illustrate their dependence on conduit inclination. For liquid viscosities of 0.001 and 0.09 Pa s (with $N_f = 30\,000$ and 340, respectively), the difference in viscosity does not appear to affect the velocity results, which lie close to the empirical curve of Zukoski (1966) and demonstrate velocity increases of up to 50% in inclined tubes. Ascent velocities in a liquid with viscosity of 0.9 Pa s ($N_f = 34$) are significantly lower, pointing to the increasing importance of viscous drag for values of N_f low-

er than those included in the Zukoski (1966) curve.

3.3. Slug approaching the liquid surface

Low-amplitude pressure oscillations were frequently observed as the slug approached the surface. Fig. 5a illustrates oscillations detected in front of the nose of a slug in water (0.001 Pa s). The top panel in Fig. 5b shows the data of Fig. 5a after filtering with a 7–100-Hz band-pass filter. The oscillations show a marked frequency increase as the front of the bubble approaches and passes by the transducer. No similar oscillations were detected in higher-viscosity liquids in vertical tubes (Fig. 5a) or in inclined tubes (Fig. 5c), although their detection may have been hampered by higher levels of background oscillations in the latter experiments. The source of the background oscillations is unknown, but the fact that these were observed only in inclined tubes and could persist even after a slug had burst, suggests that they were probably not directly related to slug ascent. Background oscillations were absent prior to slug release and we surmise these may represent an experimental artefact associated with the removal of the gate and the apparatus suspension system for inclined tubes.

The data in Fig. 5c illustrate the spatial distribution of pressure in front of the bubble in inclined tubes. The pressure sensor located near the top of the tube (sensor 163PC 2 in Fig. 1) recorded pressure spikes before the noses of passing slugs. These spikes represent dynamic pressure changes associated with the movement of the liquid out of the path of the slug. The spike duration ($\sim$150 ms in 0.001-Pa-s liquid) suggests that the pressure transient originates within a short distance ($\sim 1D$) in front of the slug, in agreement with previous calculations and measurements of the liquid velocity field ahead of a gas slug (Polonsky et al., 1999a; Bugg and Saad, 2002).

3.4. Slug burst

Processes observed to occur during slug bursts are illustrated schematically in Fig. 6. In vertical tubes and low-viscosity liquids, upon arrival at the surface the slug nose flattens out as liquid drains rapidly to form a membrane. In several experiments, an upward flexure of this membrane was observed in a single video frame before the membrane returned to a flat, horizontal form. In a 0.9-Pa-s liquid, the viscosity appeared to be sufficient to significantly hinder drainage from the region directly in front of the gas slug. As a result, the liquid surface domed on approach of the slug nose and a curved membrane was formed initially, often lasting for several video frames (>0.08 s in Fig. 6b). Liquid was observed to drain from it and from the tube walls below it and, in most cases, the membrane completely disappeared during the 0.04-s interval separating successive video frames. In inclined tubes, surface tension maintained the membrane perpendicular to the tube wall (Fig. 6c) and the membrane gradually moved

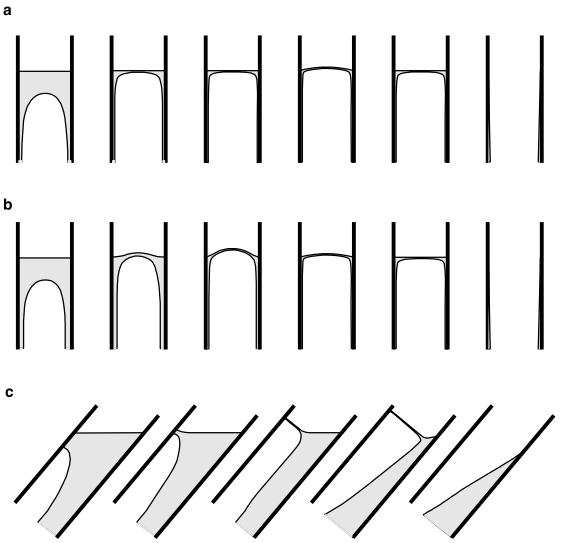

Fig. 6. Sketches of slug arrival and ensuing burst at the liquid surface. (a) Typical processes observed during the burst of a slug in a 0.001-Pa-s liquid. (b) Processes observed in a 0.9-Pa-s liquid. Due to increased liquid viscosity, liquid drainage from the region in front of the slug is slowed. This produces a more pronounced protruding nose as the slug reaches the surface compared to that seen in a 0.001-Pa-s liquid. (c) Same as (b) for a tube inclined at 40°. Differences between 0.9- and 0.001-Pa-s liquids are similar to those observed in vertical tubes. Lower viscosities enhance drainage from the front of the slug. The inclination of the membrane (compared with the horizontal membrane produced in vertical tubes) also enhances membrane drainage and reduces its lifespan.

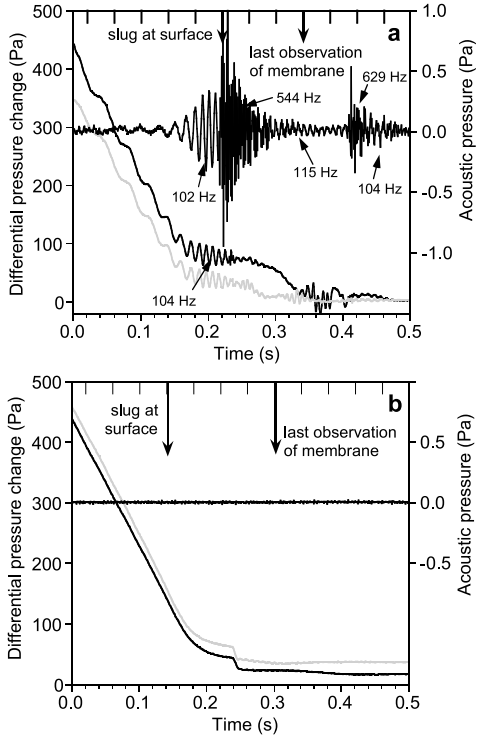

Fig. 7. Pressure changes measured near the liquid surface during the bursting of a slug. The pressure (163PC, left-hand axis) and microphone data (black, horizontal trace, centred on 0 Pa in the right-hand scale) are shown together with video observations for slugs bursting in 0.001-Pa-s (a) and 0.9-Pa-s (b) liquids. Representative frequencies are labelled, including frequencies near 100 Hz associated with longitudinal wave resonance of the air column in the open end of the experimental tube. Ticks on the top horizontal axis mark the timing of individual video frames. In (a), the frequencies of pressure oscillations detected by transducers 163PC 1 (black trace) and 163PC 2 (grey trace) are observed to increase as the slug reaches the surface (see also Fig. 5b). The oscillations are detected by the microphone as they approach its sensitivity range and the air column is stimulated into resonance. The sudden onset of frequencies >500 Hz is attributed to the production and oscillation of a membrane at the surface. The second burst of acoustic energy is attributed to fluid sloshing at the base of the bubble after the membrane has burst. No oscillations are observed in the more viscous fluid in (b). The small steps in the 163PC data in (b) are believed to represent the bursting of the bubble. These steps always appear within $\sim$80 ms prior to the last observation of the top membrane.

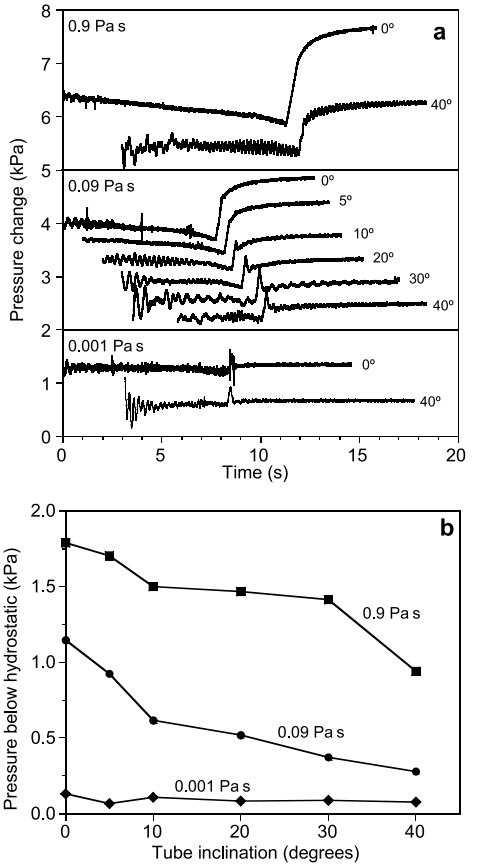

Fig. 8. Pressure changes measured at the base of the experimental tube (at transducer ASG 1 located $\sim$2 m below the liquid surface) during the bursting of gas slugs. The data are shown for different liquid viscosities and tube inclinations. Each trace has been offset vertically and horizontally for clarity. The arrival of the slug at the surface coincides with the step-like pressure increase in each trace. The shapes of the pressure signals induced as the slug reaches the surface, range from smooth large-amplitude pressure increases in vertical tubes and high-viscosity liquids (due to the gradual slumping of the liquid coating the walls of the tube), to sharp smaller-amplitude pressure spikes in inclined tubes and low-viscosity liquids (due to the termination of dynamic processes). (b) Maximum amplitude of the sub-static pressure measured at ASG 1 (i.e. the difference between the pressure recorded just prior to the slug arriving at the surface and the pressure recorded at the end of the experiment), plotted for a range of tube angles and three liquid viscosities.

upward as the liquid drained past the body of the slug. The membrane inclination enhanced fluid drainage from it so that full-tube width membranes were seldom observed in inclined tubes.

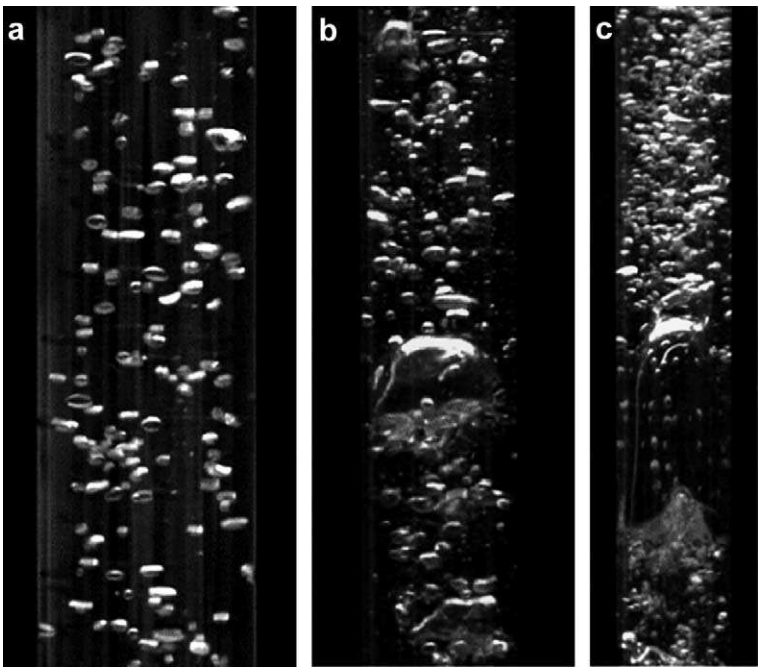

Fig. 9. Examples of flow regimes observed during continuously supplied two-phase flow. (a) Bubbly flow. (b) Transitional flow. (c) Slug flow. The images are obtained at different magnifications, but each represents a view of the same tube with external diameter of 4 cm.

Pressure oscillations were detected by the microphone and 163PC sensors during the generation and destruction of the membrane. Oscillation amplitudes were largest in low-viscosity liquids, and appeared to be heavily damped in higher-viscosity liquids. Fig. 7a shows the 163PC and microphone data recorded during a slug burst in a vertical tube filled with a 0.001-Pa-s viscosity liquid. The low-frequency oscillations discussed in the previous section can be observed in the 163PC data as the slug nose approaches the surface. The oscillation frequency increases up to about 100 Hz as a domed membrane briefly forms and oscillations begin to be picked up by the microphone. As the membrane flattens, the microphone picks up higher frequencies in the range 540–680 Hz attributed to oscillations of the membrane itself. These higher frequencies, however, were often swamped by stronger signals with frequencies near 100 Hz (Fig. 7a) attributed to acoustic resonance of the air column in the open end of the tube. No oscillations were detected in a similar experiment carried out with a 0.9-Pa-s liquid (Fig. 7b), suggesting an overdamped system.

The steps in the 163PC data in Fig. 7b are believed to be related to the bursting of the membrane. In experiments carried out with dyed water to increase the visibility of the liquid, the pressure steps always occurred within the two frames (0.08 s) preceding the observed disappearance of the meniscus ring surrounding the membrane. Accordingly, we interpret the pressure drop as resulting from the initial bursting of the membrane, which releases the small surface tension pressure remaining in the expanded slug. The time delay before the disappearance of the meniscus ring therefore reflects the time required to completely collapse the membrane and drain the meniscus ring. In experiments with water in vertical tubes, the pressure steps ranged between 5 and 7 Pa, close to the 7-Pa excess pressure calculated for a flat bubble top surface pulled downward by surface tension. Smaller pressure steps were measured in experiments conducted with water in inclined tubes (near 4 Pa in a tube inclined at 45°)

and larger steps were observed for higher-viscosity liquids (~18 Pa in a 0.9-Pa-s liquid), suggesting that there may also be a pressure contribution due to the non-negligible mass of liquid in the membrane. If this is assumed to account for ~11 Pa in the 0.9-Pa-s liquid, then the implied membrane thickness would be ~1 mm, a reasonable value for a liquid with this viscosity.

Pressure changes were also recorded by the ASG sensors along the tube during the bursting of slugs at the liquid surface (Fig. 2a,c), with the sharp onset of the pressure increases coinciding with the nose of the slug arriving at the surface of the liquid. The shape of the pressure signal was observed to vary with both liquid viscosity and tube angle. The pressure signals (Fig. 8a) range from a large-magnitude, smoothly increasing pressure in high-viscosity liquids in vertical tubes, to relatively smaller, sharp pulses in low-viscosity liquids in inclined tubes. The diversity of pressure waveforms between these extremes is illustrated in the middle panel of Fig. 8a for a range of tube inclinations and fixed liquid viscosity of 0.09 Pa s. In all experiments, a sub-static pressure was recorded during slug ascent, followed by a return to hydrostatic pressure after the slug had burst. The maximum magnitudes of the sub-static pressures recorded are shown in Fig. 8b.

The large magnitudes of the pressure changes observed in high-viscosity liquids in vertical tubes reflect the relative importance of dynamic losses in the liquid film around the gas slug as it ascends. The high liquid viscosity also prevents rapid drainage of this film, resulting in a slow and smooth pressure increase after the slug burst (Figs. 2a,c and 8a). In inclined tubes, the gas slug is concentrated against the upper wall of the tube, effectively increasing the thickness of the liquid film which flows past below the slug. As a result, dynamic losses due to the liquid viscosity are decreased in this region of flow (due to decreased liquid velocities) and drainage after the slug burst is more rapid. This accounts for the smaller magnitudes and decreased durations of the pressure increases observed in a 0.9-Pa-s liquid in a tube inclined at 40° (Fig. 8a).

Only a very small overall pressure increase is observed in low-viscosity liquids. This minimal

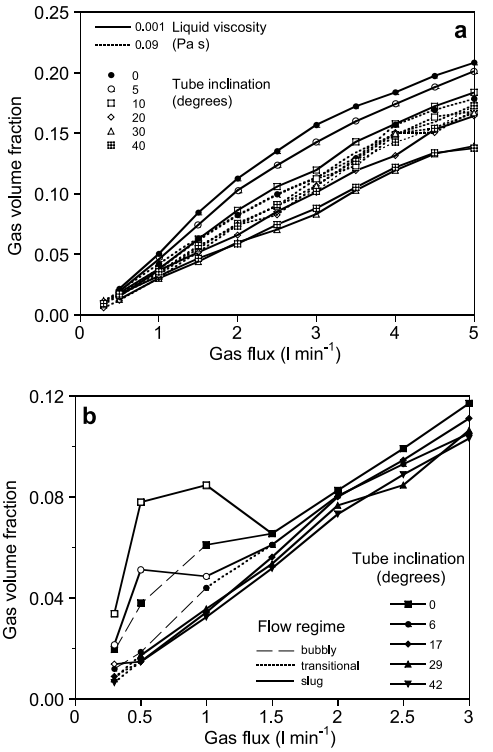

Fig. 10. Results of gas-volume fraction measurements carried out during continuous gas supply experiments. (a) Gas-volume fractions measured over a range of tube inclinations for liquid viscosities of 0.001 and 0.09 Pa s. (b) Data from similar experiments carried out with a coarser bubbler. Different flow regimes are indicated by dashed lines (bubbly flow), dotted lines (transitional flow), and bold lines (slug flow). The open symbols show the overall results obtained when a surface foam layer is present and is included in the gas-volume fraction calculation. The foam is taken into account by adding the thickness of foam to the height of the liquid surface measured during the flow.

increase reflects the small dynamic losses due to viscosity in the flowing liquid. Superimposed on this increase, however, is a ~400-Pa pressure pulse, which exceeds hydrostatic pressure and therefore cannot be the result of a static effect. We interpret this pulse as reflecting the sudden collapse of the liquid velocity field in front of the slug upon its arrival at the surface of the liquid. During slug ascent, volume conservation requires that the liquid immediately ahead of the slug must accelerate downward to flow past the slug. This annular liquid film must then decelerate

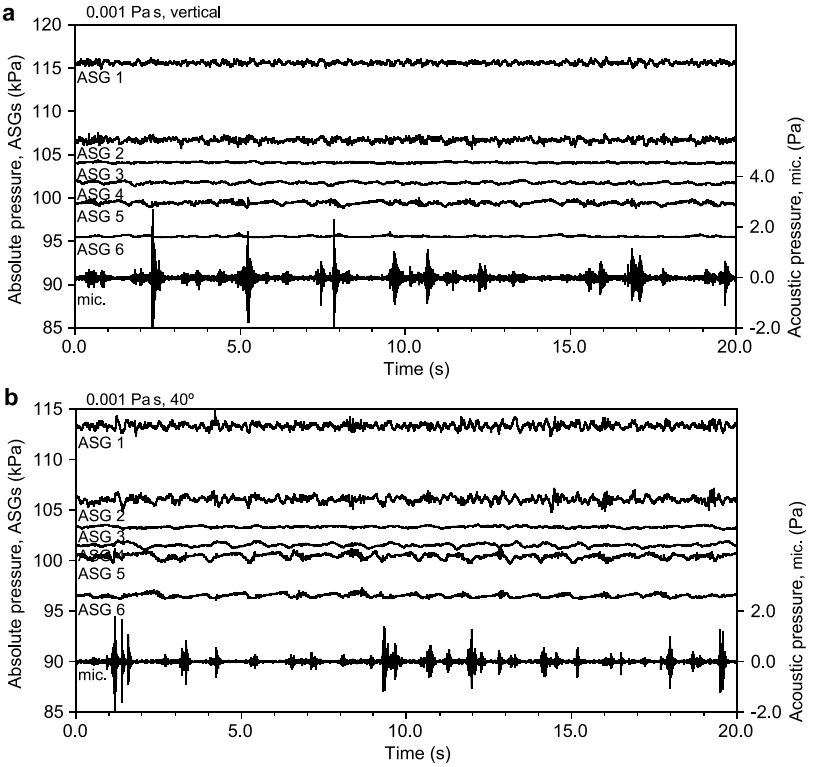

Fig. 11. ASG and microphone data recorded during continuous gas supply experiments with water (0.001 Pa s). (a) Vertical tube. (b) Tube inclined at 40°. Ramps in the ASG data indicate the approach and passage of gas slugs past the sensors.

back to stationary below the slug. For a slug with ascent velocity U and radius r_s, the volume flux is $\pi r_s^2 U$, corresponding to a downwards flowing liquid mass flux of $\rho\pi r_s^2 U$. If the slug occupies $\sim$90% of the cross-sectional area of the tube, the liquid film must accelerate up to $10U$, effectively inducing a reaction force of $10\rho\pi r_s^2 U^2$ (mass flux $\times$ velocity change) on the stationary liquid above the slug.

To decelerate this liquid back to stationary, a force with the same magnitude but opposite direction is required. Neglecting viscous dissipation and considering only liquid inertia, the downward-flowing annular film exerts this force on the stationary liquid below the slug. During slug ascent, these equal and opposite forces above and below the slug cancel each other out, however, when the slug reaches the surface, the force above the slug disappears shortly before the force decelerating the liquid below the slug. Over the cross-sectional area of the tube this translates into a pressure pulse with magnitude $40\rho U^2(r_s/D)^2$. For water (1000 kg m^{-3}) and a slug velocity of $\sim$0.2 m s^{-1}, this yields 360 Pa.

We believe that the agreement between this estimate and the data shown in Fig. 8a provides strong support for the viability of such mechanism in the generation of the super-static pressure spikes recorded at the arrival of inertial slugs at the liquid surface. The only other process capable of generating pressures larger than static is the jet recoil from the bursting slug. However, the super-static pressures measured in the slugs were observed to be small (Fig. 7), indicating that jet recoil has a negligible effect in our experiments.

4. Experiments with a continuous supply of gas

Experiments in which gas was supplied contin-

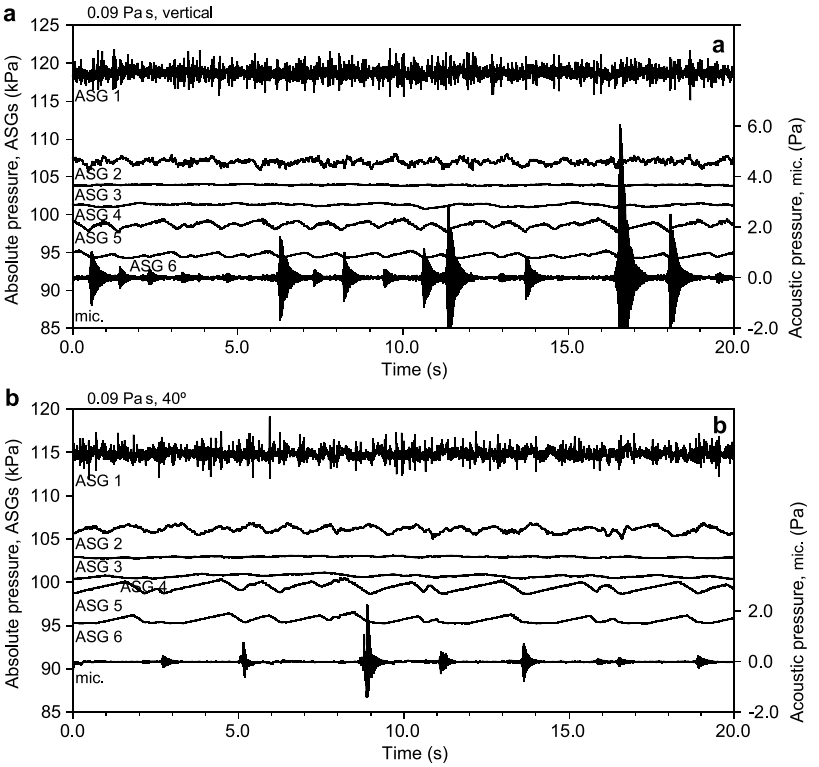

Fig. 12. ASG and microphone data recorded during continuous gas supply experiments with a sugar solution (0.09 Pa s). (a) Vertical tube. (b) Tube inclined at 40°. The time delays (<0.5 s) between individual peaks in the sawtooth signals recorded by ASG 6 and the corresponding onsets of acoustic signals recorded by the microphone are measures of the times taken by the noses of individual slugs to travel from the depth of ASG 6 to the surface of the liquid.

uously to the base of the liquid column were only carried out with two different solutions, namely tap water (0.001 Pa s) and a sugar solution with a viscosity of 0.09 Pa s. At higher viscosities, the bubblers used could not produce small dispersed bubbles, but generated only large, slug-like bubbles. Therefore, the transition between bubbly and slug flow was not investigated in the 0.9-Pa-s solution with the apparatus available for these experiments.

4.1. Flow regimes

A series of experiments were carried out over a range of tube inclinations and gas-supply rates to investigate the dependence of flow regime and average gas-volume fraction on these parameters. An average gas-volume fraction was calculated from the average height of the liquid surface measured during two-phase flow compared to the height of the liquid surface measured during zero gas flux. Bubbly, transitional, and slug flow regimes were observed over a range of gas fluxes of 0.3–5 l min^{-1} (either measured at, or calibrated to atmospheric pressure). These regimes were identified by visual observation and typical examples are illustrated in Fig. 9. The bubbly regime is characterised by small, well dispersed ascending bubbles with a relatively narrow size distribution (Fig. 9a). The transitional regime is marked by the appearance of bubble clusters and considerably larger bubbles resulting from coalescence of smaller bubbles (Fig. 9b). In other studies, the onset of the transitional regime has been identified by the presence of a bimodal bubble size distribution suggestive of bubble coalescence (Krussenberg et al., 2000). The slug flow regime is characterised by larger bubbles with diameters similar to

that of the confining tube. These bubbles are longer than they are wide (Fig. 9c).

Fig. 10 shows the average gas-volume fraction measured as a function of gas flux and tube inclination. The gas-volume fraction decreases with increasing tube inclination (Fig. 10a). The effect is stronger in a low-viscosity (0.001 Pa s) liquid than for a higher-viscosity (0.09 Pa s) liquid. In these experiments, the flow regimes were dominantly slug flows, with some transitional and bubbly flows at the lowest gas fluxes. Fig. 10b shows similar data for a 0.09-Pa-s sugar solution aerated with a coarser ceramic bubbler to demonstrate flow regime transitions. The coarser bubbler proved more efficient at producing bubbles in higher-viscosity liquids and in generating enhanced regions of bubbly flow. Different flow regimes are indicated by the dashed, dotted, and bold lines in Fig. 10b. The production of a foamy head was also observed at some flow rates (Fig. 10b). In our experiments, foam generation was a result of bubbly flow conditions and the foam head was destroyed by the onset of transitional and slug flow and greatly reduced by tube inclination. This behaviour is in contrast to the results of Seyfried and Freundt (2000), who report a gradual aeration of their liquid column during slug flow due to a downflow of bubbles entrained during slug burst.

4.2. Pressure measurements

Examples of ASG and microphone pressure recordings obtained over a 20-s interval during continuous gas supply are shown in Fig. 11 for a liquid viscosity of 0.001 Pa s and tube inclinations of 0 and 40°. Near the region of bubble generation, pressure changes are dominated by this process, resulting in a relatively noisy and high-frequency signal (see trace at ASG 1). The data recorded at ASG 1 are relatively well correlated with those recorded at ASG 2, but at ASG 3 and higher up the fluid column most of this high-frequency signal is gone. Pressure changes recorded at ASG 3–5 are increasingly dominated by a sawtooth signal with upgoing ramps reflecting the increasing static pressures due to slug expansion during slug ascent. The arrival of most (but not all) of the slugs at the surface and their subsequent bursting is indicated by the microphone. If the amplitude of pressure change at ASG 5 and 6 is viewed as a proxy for slug size, then the acoustic energy released at bursting does not appear to be well correlated with the slug size. The pressure data collected in vertical and inclined tubes appear to be relatively similar, however, inclined tubes generated less acoustic energy than vertical tubes.

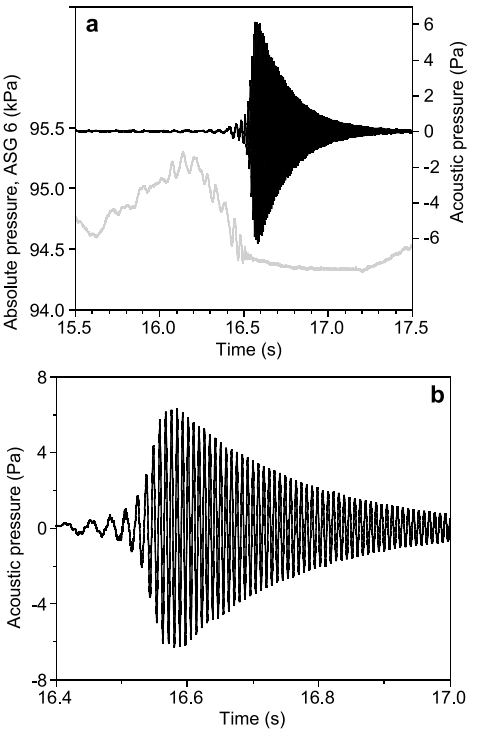

Fig. 13. (a) ASG 6 (grey) and microphone (black) data recorded during a slug burst event in a continuous gas flow experiment. The increasing then decreasing pressure recorded by ASG 6 is due to the increasing static pressure as the expanding slug approaches the transducer, then decreasing static pressure as the gas slug passes the transducer. The pressure oscillations detected by the ASG 6 transducer as the slug approaches the surface are considerably enhanced compared to those measured during the ascent of single slugs. (b) Microphone data magnified to illustrate the quasi-monochromatic characteristics of the signal with frequency near 120 Hz. This signal is consistent with longitudinal wave resonance of the air column in the open end of the experimental tube.

Data collected during similar experiments with a 0.09-Pa-s viscosity solution are shown in Fig.

12. The results are qualitatively similar to those obtained in experiments with water (0.001 Pa s), but display larger pressure variations. Specifically, the magnitudes of acoustic pressure changes are up to three times larger than those observed during the experiments with water. The higher-amplitude ASG data indicate that the slugs are larger and less frequent than in the 0.001-Pa-s liquid. The number of slugs per unit time also depends on the tube inclination. Over the 20-s interval, 27 slugs were observed in a 0.001-Pa-s liquid in a vertical tube vs. 21 slugs for the same liquid in a tube inclined at 40°. In contrast, 22 slugs were observed over the same interval in a 0.09-Pa-s liquid in a vertical tube vs. 13 slugs for the same liquid in a tube inclined at 40°.

Fig. 13 shows the details of a slug burst in a vertical tube filled with a 0.09-Pa-s liquid. Fig. 13a shows data from ASG 6 and the microphone during the slug burst near 16.5 s. The ASG 6 data show pressure oscillations as the slug approaches the surface. These oscillations are one order of magnitude larger than those recorded during the ascent of a single slug. This is interpreted to reflect the continuous nature of the flow, which generates many sources of oscillations and enhances the stimulation of the resonant frequencies of the ascending slugs. Similarly, the microphone data (see detail in Fig. 13b) show much larger amplitudes than observed in individual slugs. The oscillation frequency near 120 Hz in Fig. 13b is consistent with longitudinal acoustic resonance of the air in the open end of the tube. Frequencies directly related to membrane oscillation were not observed.

The continuous gas supply experiments show sub-static pressures at the base of the tube similar to those observed during single slug experiments. The magnitudes of the pressure changes below static were largest for viscous liquids in vertical tubes aerated with high gas fluxes ($\sim$1.5 kPa in a 0.09-Pa-s liquid aerated with a gas flux of 5 l min^{-1}) and decreased with increasing tube inclination ($\sim$700 Pa in a 0.09-Pa-s liquid aerated with a gas flux of 5 l min^{-1} in a tube inclined at 40°), decreasing gas flux ($\sim$350 Pa in a 0.09-Pa-s liquid aerated with a gas flux of 1 l min^{-1} in a vertical tube), and decreasing liquid viscosity ($\sim$240 Pa in a 0.001-Pa-s liquid aerated with a gas flux of 5 l min^{-1}in a vertical tube).

5. Discussion

Our experiments demonstrate the importance of tube inclination in promoting bubble coalescence and hence slug formation by locally enhancing the gas-volume fraction on the upper wall of the tube. For any reasonably long conduit, only very small angles of inclination could therefore result in transitional, if not slug, flow. Once a large bubble is produced, its increased ascent velocity will allow it to continue to grow by enhanced coalescence. Even in situations with multiple rising slugs of similar sizes, it has been demonstrated that slugs continue to coalesce if their separation distance is less than 10–20D (Pinto and Campos, 1996; Polonsky et al., 1999a).

The inclined conduit imaged at Stromboli volcano (Chouet et al., 2002) could thus effectively control the production of gas slugs by enhanced coalescence rather than by the collapse of foam rafts. The slugs generated in this manner will rise more rapidly and are likely to be larger than those expected in vertical conduits. For a conduit inclined at 30°, slug ascent velocity is likely to be increased by $\sim$40%. Taking this velocity increase into account may help reconcile differences between previously calculated slug ascent velocities and those determined from infrasonic data (Ripepe et al., 2001). The pressure data in Fig. 8 also suggest that tube inclination enhances inertial effects in single-slug flows. By concentrating the slug on the upper conduit wall and increasing the thickness of the downward-flowing liquid film, tube inclination reduces dynamic losses due to viscosity within this backflow. Consequently, slugs ascending inclined tubes should be less susceptible to factors such as wall roughness.

The flow regime produced may have further consequences than simply determining the size of bubbles bursting at the surface. The ascent of small bubbles is significantly less efficient at liquid mixing than the ascent of slugs. In a magma, this could allow sufficient cooling of the top surface to form a carapace. Slug flow is also more efficient at

disrupting the surface, as demonstrated during some of the continuous supply experiments in which foam layers, having accumulated during bubbly flow, were destroyed when the flow regime was changed to slug flow. Liquid mixing by slug ascent is particularly enhanced in inclined conduits, where a complete circulatory system can be observed, with the liquid near the lower surface of the conduit being drawn downwards. It is therefore possible that inclined conduits favour typical Strombolian-type activity, whereas a nearly vertical conduit might periodically induce more violent explosions caused by the disruption of a cool carapace or a foam layer with a significant yield strength. In essence, conduit inclination should be considered as having the potential for considerable control over eruptive style.

5.1. Forces and pressure changes

The pressure fluctuations recorded during the ascent of individual gas slugs include contributions from both static and dynamic processes. The production of gas slugs at basaltic volcanoes is frequently ascribed to the collapse of an accumulating foam layer (Jaupart and Vergniolle, 1989; Chouet et al., 1997; Ripepe and Gordeev, 1999). Combining the pressure changes caused by foam layer collapse with our data may account for the process believed to be responsible for VLP seismic data at Stromboli (Chouet et al., 2002).

Numerical investigations of foam collapse as a possible seismic source at Stromboli were previously carried out by Ripepe and Gordeev (1999). Considering only static effects, Ripepe and Gordeev (1999) concluded that pressure changes would only be small ($\sim$80–800 Pa) for 'free coalescence' of bubbles in basaltic systems. However, Chouet et al. (2002) demonstrated the possibility of generating much larger pressure changes (up to 10^6 Pa) if dynamic effects of bubble growth are also accounted for.

If significant super-static pressures can be generated, VLP seismic signals may be related to the whole-scale translational motion of the liquid column on top of the slug. As the gas expands in order to adjust to static pressure, a downward-directed single force is initially produced as a reaction force to the upward accelerating mass of liquid displaced by the piston-like action of the slug (Takei and Kumazawa, 1994). As the slug starts to accelerates upwards, magma must also accelerate downward to fill the void left by the escaping gas. The downward acceleration of the liquid film which is produced around the slug generates a reaction force in the form of an upward-directed single force. When the slug reaches the surface, this latter force is reversed as the downward-flowing liquid mass in the film is decelerated and a single downward force is exerted. This process was described from the viewpoint of accelerating and decelerating liquid on the side of the ascending slug in Section 3.4 and is believed to be responsible for the pressure pulses recorded during the bursting of slugs in low-viscosity liquids (see lower panel in Fig. 8a).

As the slug rises, the viscosity of the down-flowing magma exerts a shear stress on the conduit walls. This viscous drag is responsible for the generation of the sub-static pressures measured below the slug in our experiments (Figs. 2c and 8b). A simple way to envisage this process is to assume that a section of the liquid film flowing past the bubble essentially goes into free fall and reaches its terminal velocity as determined by the wall friction and liquid viscosity (Wallis, 1969). This volume of liquid in the shape of an annular film of 'equilibrium' thickness, is supported by the tube wall (Brown, 1965) and exerts a downward force on it, due to its mass. This liquid mass is thus effectively removed from the measured hydrostatic head, and results in the sub-static pressures measured below the slug. Even if the liquid in the down-flowing film around the slug never reaches its terminal velocity, this mechanism still applies because of the shear stress exerted by the flowing liquid on the walls of the tube.

An accurate assessment of the magnitude of this pressure drop requires a calculation of the full flow field around the slug. Such calculation is beyond the scope of the present study, which is limited to a simplified extrapolation of our results to parameters consistent with a basaltic system. The mass of the liquid film may be estimated under the assumption that the pressure drop is

due to a liquid film of 'equilibrium' thickness that is present over the entire length of the slug. This assumption neglects the non-uniform thickness of the film and also disregards the fact that the film is not fully supported by the wall. However, these are opposing factors whose effects tend to cancel each other out and become less important with increasing slug lengths. Brown (1965) gave an equation for the equilibrium thickness, δ_0, of the film in a vertical tube as:

$$\delta_0 = \frac{-1+\sqrt{1+ND}}{N} \quad (5)$$

where:

$$N = \sqrt[3]{14.5\frac{\rho^2 g}{\mu^2}} \quad (6)$$

For the liquid viscosities considered in our experiments (0.9, 0.09 and 0.001 Pa s), this yields $\delta_0 = 6$, 3, and 0.8 mm, respectively. Using these values of δ_0 and assuming a 0.2-m-long slug, the decreases in hydrostatic pressure associated with the removal of this liquid from the static head are 1700, 830 and 170 Pa. Although Eq. 5 was developed from equations for inertial slugs, adjusted to account for viscous effects within a laminar, down-flowing film (Brown, 1965), conditions that are not all met in our experiments, these estimates are in reasonable agreement with the measured values of 1800, 1100 and 130 Pa in Fig. 8b. For a basaltic system with $D = 2$ m, $\mu = 400$ Pa s and $\rho = 2600$ kg m^{-3} (Vergniolle and Brandeis, 1996), a liquid film with thickness of 0.3 m is calculated which, for a 10-m-long slug, implies a mass of 5×10^4 kg, yielding a pressure drop on the order of 100 kPa. Accordingly, during slug ascent, the 'source' region would experience a sub-static pressure of $\sim$100 kPa and the conduit walls would experience a downward force of $\sim5\times10^5$ N. Although the magnitudes of these pressures and forces are two and three orders of magnitude less than those required to interpret seismic data from Stromboli (Chouet et al., 2002), the crude nature of our calculations suggests that their importance should not necessarily be discounted.

As shown in Fig. 8, pressure changes triggered by the bursting of the gas slug at the surface depend on the inclination of the conduit, and may vary from a gradual increase of pressure back to hydrostatic to a sharp pressure pulse larger than static. Such variations may be considered to reflect slug dynamics ranging from inertial behaviour (small sub-static pressures during slug ascent and a super-static pressure pulse during bursting) to viscous behaviour (large-magnitude sub-static pressures during slug ascent and no super-static pressure pulse on bursting). The pressure changes indicative of inertial behaviour are thought to be present in the data of Ripepe et al. (2001), who produced gas slugs from foam collapse (see fig. 12 in Ripepe et al., 2001). If a basaltic system produces slugs that are dominantly inertially-controlled, then the magnitude of the pressure pulse generated upon the arrival of a slug at the surface is likely to be on the order of 10^4 to 10^5 Pa ($\rho \approx 2600$ kg m^{-3} and $0.6 < U < 2$ m s^{-1}; Section 3.4). However, this is also likely to be combined with another pulse due to the jet recoil force (Kanamori et al., 1984; Chouet et al., 1997) due to a dynamically-produced super-static pressure in the slug.

5.2. Pressure oscillations

Seismic and acoustic data from basaltic volcanoes display a range of characteristic periods associated with the source process (e.g. Chouet, 1996; Chouet et al., 2002). During our experiments, pressure oscillations (Table 2) were gener-

Table 2
Pressure oscillations recorded

Source	Observed frequency	Duration
Turbulent flow in the slug wake	$\sim$19 Hz	duration of slug ascent
Longitudinal oscillations of the slug as it approaches the surface	$\sim$12 to 30 Hz	<1 s
Bubble membrane oscillation	$\sim$540 to 680 Hz	<100 ms
Longitudinal resonance of the air column above the liquid	$\sim$100 to 120 Hz	exponential decay lasting up to $\sim$1 s.

ated during slug release (Fig. 2b), in the slug wake (Fig. 3), as slugs approached the surface (Fig. 5), and during and after slugs burst at the surface (Figs. 7 and 13). Vergniolle et al. (1996) considered several different modes of gas slug oscillation to account for acoustic data recorded during explosions at Stromboli. One of the modes they considered is the longitudinal oscillation of an ascending slug in a tube. The oscillation frequencies observed in our experiments are consistent with longitudinal oscillations of slugs under atmospheric pressure as the slug approaches the surface of the liquid. This process effectively represents the 'bouncing' of the liquid column on top of a gas spring, with frequency given by (Vergniolle et al., 1996):

$$f_L = \frac{1}{2\pi}\sqrt{\frac{\gamma P_g}{\rho L_{eq} H_l}} \tag{7}$$

where γ is the ratio of specific heats of the gas ($\gamma = 1.3$ for air), L_{eq} is the equilibrium bubble length, H_l is the depth of the slug in the liquid, and P_g is the gas pressure in the slug. For slugs under atmospheric pressure and with equilibrium lengths of 8 and 24 cm, released under water columns 2 m in height, our measured oscillation frequencies are 4.7 and 2.8 Hz, in close agreement with the values of 5.0 and 2.9 Hz calculated with Eq. 7. These oscillations (Fig. 2b) display peak-to-peak amplitudes of up to 45 kPa, which are three orders of magnitude larger than the change in static pressure expected if compression of the gas slug is calculated without consideration of the dynamic terms. Dynamic pressures were also observed below the bubble (at ASG 1 in Fig. 2b), where static pressure does not change after the release of the slug. This type of oscillation could be induced in a basaltic system due to foam collapse and would greatly enhance pressure changes associated with this process.

The increasing frequency of oscillations observed as slugs approach the surface can also be modelled as longitudinal bubble oscillations. The white line in the spectrogram in Fig. 5b represents the frequency calculated from Eq. 7 assuming a bubble length of 0.22 m, an ascent velocity 0.2 m s^{-1}, and an arrival time at the surface of 13.79 s (taken from the video data). Given that Eq. 7 does not account for the domed top of the slug which, at shallow depths, will be of similar size to the head of liquid above it, the calculated results are in remarkable agreement with the data. These oscillations are observable for ~ 0.7 s before the slug bursts, representing a distance of $\sim 4D$. Previous work suggested that the local liquid velocity field in front of a slug extends no further than D in front of the nose, and is probably confined within a scale closer to $0.5D$ (Polonsky et al., 1999b; Bugg and Saad, 2002). Therefore, it seems unlikely that these oscillations are being triggered by the interaction of the liquid velocity field with the liquid surface. It is more probable that they become detectable as their amplitude increases due to the decreasing mass of oscillating water above the slug.

Vergniolle et al. (1996) also suggested that different frequencies within their acoustic data might be accounted for by shape oscillations of a bubble nose, vibrations of the bubble membrane produced at the surface, and kinematic waves in the draining fluid films after the bubble has burst. During our experiments with single gas slugs we did not detect any shape oscillations of bubble noses, although extreme shape distortions were observed during the continuous gas supply experiments due to turbulence in the liquid the slugs were passing through. Single slugs did demonstrate membrane oscillations and kinematic waves in the draining film, although no recorded pressure signals can be ascribed to the kinematic waves.

The membrane oscillations considered by Vergniolle et al. (1996) (their 'bubble oscillation mode') were radial movements of a domed membrane allowed to move across a liquid surface. However, in the experiments described here, membranes were bounded by the tube and are therefore considered as 'drum skins' rather than as oscillating bubbles. The frequency, f_m, of the fundamental axial mode of oscillation for this geometry is given by (Morse and Ingard, 1968):

$$f_m = 0.38274\frac{1}{a}\sqrt{\frac{T}{\rho_s}} \tag{8}$$

where T is the tension force per unit length of

edge, ρ_s is the surface mass density, and a (0.019 m) is the membrane radius. The membranes produced by slugs are bounded by an upper and lower interfacial surface, hence $T = 2\sigma$, and the frequencies ascribed to their oscillation range between $\sim$540 and 680 Hz. Defining the surface mass density as ρt_m, where t_m is the membrane thickness, and using $\rho = 1000$ kg m^{-3} and $\sigma = 0.07$ N m^{-1} for water, we obtain from Eq. 8 membrane thicknesses of 200 and 120 nm for the frequencies of 540 and 680 Hz, respectively. These values are small but not unreasonable for bubble membrane thicknesses, and we interpret these frequencies as being due to this fundamental axial oscillation mode. However, in many experiments these oscillations were swamped by those associated with tube resonance ($\sim$100–120 Hz, depending on the exact configuration of the tube and the liquid level in it).

The final oscillatory source we consider is the slug wake, during the passage of which pressure oscillations with frequencies near 19 Hz were recorded in 0.001-Pa-s liquid (Fig. 3). At this viscosity, the slugs rose with Reynolds numbers of $\sim$8000, placing them well into the region of turbulent wakes ($Re > 300$) as defined by Campos and Guedes de Carvalho (1988). This is in agreement with visual observations of the turbulent slug wake, much of which was marked by a train of entrained bubbles behind the slug. During these experiments, the base of the slug was also observed to constantly change shape in a sloshing manner. Although we cannot attribute any pressure changes to this process, Polonsky et al. (1999a) showed that the amplitudes of pressure fluctuations associated with such wakes increase with slug length, and that the frequencies of pressure fluctuations depend on slug length only for bubbles shorter than $\sim 10D$. Slugs in some basaltic systems might be expected to rise with Reynolds numbers > 300, so turbulent wakes may provide seismic sources or energy to stimulate resonance of other parts of the system.

6. Summary

Pressure measurements carried out during the ascent of gas slugs in liquid-filled tubes demonstrate the importance of both static and dynamic pressure changes. Conduit inclination promotes bubble coalescence and the slug flow regime in two-phase flow, increasing slug size and slug ascent velocity at the expense of the frequency of occurrence of slugs as compared to identical gas fluxes in vertical tubes. By concentrating gas on the upper wall of the tube and increasing the thickness of the liquid film flowing around the lower surface of the slug, tube inclination effectively increases the importance of inertial over viscous effects within the flow.

The ascent of bubbles and slugs provides a rich source of pressure oscillations (Table 2). Different frequencies are detected at different heights along the fluid column in continuous gas-supplied flow experiments. Near the surface, pressure oscillations are dominated by changes in the static head and by longitudinal oscillations of the gas slugs. The frequency of the latter oscillations increases as the slugs approach the surface.

Acknowledgements

We are grateful to J. Bailey and K. Courtney for assistance during some of the experiments and to G. Ryan for useful discussions. M.R.J. was supported by The Leverhulme Trust (F/00 185A), and equipment was funded by The Royal Society. We thank E. Calder and R. Seyfried whose helpful comments improved this manuscript.

References

Arciniega-Ceballos, A., Chouet, B.A., Dawson, P., 1999. Very long-period signals associated with vulcanian explosions at Popocatepetl Volcano, Mexico. Geophys. Res. Lett. 26, 3013–3016.

Blackburn, E.A., Wilson, L., Sparks, R.S.J., 1976. Mechanics and dynamics of Strombolian activity. J. Geol. Soc. London 132, 429–440.

Brown, R.A.S., 1965. The mechanics of large gas bubbles in tubes I. Bubble velocities in stagnant liquids. Can. J. Chem. Eng. 43, 217–223.

Bugg, J.D., Saad, G.A., 2002. The velocity field around a Taylor bubble rising in a stagnant viscous fluid: Numerical

and experimental results. Int. J. Multiphase Flow 28, 791–803.

Campos, J.B.L.M., Guedes de Carvalho, J.R.F., 1988. An experimental study of the wake of gas slugs rising in liquids. J. Fluid Mech. 196, 27–37.

Cheng, H., Hills, J.H., Azzorpardi, B.J., 1998. A study of the bubble-to-slug transition in vertical gas-liquid flow in columns of different diameter. Int. J. Multiphase Flow 24, 431–452.

Chouet, B.A., 1988. Resonance of a fluid-driven crack: Radiation properties and implications for the source of long-period events and harmonic tremor. J. Geophys. Res. 93, 4375–4400.

Chouet, B., 1992. A seismic model for the source of long-period events and harmonic tremor. In: Gasparini, P., Scarpa, R., Aki, K. (Eds.), Volcanic Seismology. IAVCEI Proc. Volcanol. 3, Springer, Berlin, pp. 133–156.

Chouet, B.A., 1996. Long-period volcano seismicity: Its source and use in eruption forecasting. Nature 380, 309–316.

Chouet, B.A., Page, R.A., Stephens, C.D., Lahr, J.C., Power, J.A., 1994. Precursory swarms of long-period events at Redoubt Volcano (1989–1990), Alaska: Their origin and use as a forecasting tool. In: Miller, T.P., Chouet, B.A. (Eds.), The 1989–1990 Eruptions of Redoubt Volcano, Alaska. J. Volcanol. Geotherm. Res. 62, 95–135.

Chouet, B., Saccorotti, G., Martini, M., Dawson, P., De Luca, G., Milana, G., Scarpa, R., 1997. Source and path effects in the wave fields of tremor and explosions at Stromboli Volcano, Italy. J. Geophys. Res. 102, 15129–15150.

Chouet, B., Saccorotti, G., Dawson, P., Martini, M., Scarpa, R., De Luca, G., Milana, G., Cattaneo, M., 1999. Broadband measurements of the sources of explosions at Stromboli Volcano, Italy. Geophys. Res. Lett. 26, 1937–1940.

Chouet, B., Dawson, P., Ohminato, T., Martini, M., Saccorotti, G., Giudicepietro, F., De Luca, G., Milana, G., Scarpa, R., 2002. Source mechanisms of explosions at Stromboli Volcano, Italy, determined from moment-tensor inversions of very-long-period data. J. Geophys. Res. (in press).

Clift, R., Grace, J.R., Weber, M.E., 1978. Bubbles, Drops and Particles. Academic Press, New York.

Fabre, J., Liné, A., 1992. Modelling of two-phase slug flow. Annu. Rev. Fluid Mech. 24, 21–46.

Gopal, M., Jepson, W.P., 1998. The study of dynamic slug flow characteristics using digital image analysis – Part I: Flow visualisation. J. Energy Res. Technol. Trans. A.S.M.E. 120, 97–101.

Jaupart, C., Vergniolle, S., 1989. The generation and collapse of a foam layer at the roof of a basaltic magma chamber. J. Fluid Mech. 203, 347–380.

Joshi, J.B., 2001. Computational flow modelling and design of bubble column reactors. Chem. Eng. Sci. 56, 5893–5933.

Kanamori, H., Given, J.W., Lay, T., 1984. Analysis of seismic body waves excited by the Mount St. Helens eruption of May 18, 1980. J. Geophys. Res. 89, 1856–1866.

Kawaji, W.R., DeJesus, J.M., Tudose, G., 1997. Investigation of flow structures in vertical slug flow. Nucl. Eng. Des. 175, 37–48.

Konstantinou, K.I., 2002. Deterministic non-linear source processes of volcanic tremor signals accompanying the 1996 Vatnajokull eruption, central Iceland. Geophys. J. Int. 148, 663–675.

Krussenberg, A.K., Prasser, H.M., Schaffrath, A., 2000. A new criterion for the identification of the bubble slug transition in vertical tubes. Kerntechnik 65, 7–13.

Kumagai, H., Chouet, B.A., 1999. The complex frequencies of long-period seismic events as probes of fluid composition beneath volcanoes. Geophys. J. Int. 138, F7–F12.

Kumagai, H., Ohminato, T., Nakano, M., Ooi, M., Kubo, A., Inoue, H., Oikawa, J., 2001. Very-long-period seismic signals and caldera formation at Miyake Island, Japan. Science 293, 687–690.

Legius, H.J.W.M., van den Akker, H.E.A., Narumo, T., 1997. Measurements on wave propagation and bubble and slug velocities in cocurrent upward two-phase flow. Exp. Therm. Fluid Sci. 15, 267–278.

Morse, P.M., Ingard, K.U., 1968. Theoretical Acoustics. McGraw-Hill, New York.

Neuberg, J., Luckett, R., Ripepe, M., Braun, T., 1994. Highlights from a seismic broadband array on Stromboli volcano. Geophys. Res. Lett. 21, 749–752.

Nicklin, D.J., Wilkes, J.O., Davidson, J.F., 1962. Two phase flow in vertical tubes. Trans. Inst. Chem. Eng. 40, 61–68.

Nishimura, T., Nakamichi, H., Tanaka, S., Sato, M., Kobayashi, T., Ueki, S., Hamaguchi, H., Ohtake, M., Sato, H., 2000. Source process of very long period seismic events associated with the 1998 activity of Iwate Volcano, northeastern Japan. J. Geophys. Res. 105, 19135–19147.

Pinto, A.M.F.R., Campos, J.B.L.M., 1996. Coalescence of two gas slugs rising in a vertical column of liquid. Chem. Eng. Sci. 51, 45–54.

Polonsky, S., Barnea, D., Shemer, L., 1999a. Averaged and time-dependent characteristics of the motion of an elongated bubble in a vertical pipe. Int. J. Multiphase Flow 25, 795–812.

Polonsky, S., Shemer, L., Barnea, D., 1999b. The relation between the Taylor bubble motion and the velocity field ahead of it. Int. J. Multiphase Flow 25, 957–975.

Ripepe, M., Gordeev, E., 1999. Gas bubble dynamics model for shallow volcanic tremor at Stromboli. J. Geophys. Res. 104, 10639–10654.

Ripepe, M., Ciliberto, S., Schiava, M.D., 2001. Time constraints for modeling source dynamics of volcanic explosions at Stromboli. J. Geophys. Res. 106, 8713–8727.

Seyfried, R., Freundt, A., 2000. Experiments on conduit flow and eruption behavior of basaltic volcanic eruptions. J. Geophys. Res. 105, 23727–23740.

Shemer, L., Barnea, D., 1987. Visualisation of the instantaneous velocity profiles in gas–liquid slug flow. Physicochem. Hydrodyn. 8, 243–253.

Shosho, C.E., Ryan, M.E., 2001. An experimental study of the motion of long bubbles in inclined tubes. Chem. Eng. Sci. 56, 2191–2204.

Takei, Y., Kumazawa, M., 1994. Why have the single force

and torque been excluded from seismic source models? Geophys. J. Int. 118, 20–30.

Vergniolle, S., Brandeis, G., 1996. Strombolian explosions 1. A large bubble breaking at the surface of a lava column as a source of sound. J. Geophys. Res. 101, 20433–20447.

Vergniolle, S., Brandeis, G., Mareschal, J.-C., 1996. Strombolian explosions 2. Eruption dynamics determined from acoustic measurements. J. Geophys. Res. 101, 20449–20466.

Wallis, G.B. 1969. One-Dimensional Two-Phase Flow. McGraw-Hill, New York.

White, E.T., Beardmore, R.H., 1962. The velocity of rise of single cylindrical air bubbles through liquids contained in vertical tubes. Chem. Eng. Sci. 17, 351–361.

Zukoski, E.E., 1966. Influence of viscosity, surface tension, and inclination angle on motion of long bubbles in closed tubes. J. Fluid Mech. 25, 821–837.